Chemistry & Biology, Vol. 11, 499–508, April, 2004, ©2004 Elsevier Science Ltd. All rights reserved. DOI 10.1016/j.chembiol.2004.03.014

ADP-Specific Sensors Enable Universal Assay of Protein Kinase Activity

Jayaram Srinivasan, Sharon T. Cload, Nobuko Hamaguchi, Jeffrey Kurz, Sara Keene, Markus Kurz, Ryan M. Boomer, Jill Blanchard, David Epstein, Charles Wilson, and John L. Diener*
Archemix Corporation
1 Hampshire Street
Cambridge, Massachusetts 02139

Summary

Two molecular sensors that specifically recognize ADP in a background of over 100-fold molar excess of ATP are described. These sensors are nucleic-acid based and comprise a general method for monitoring protein kinase activity. The ADP-aptamer scintillation proximity assay is configured in a single-step, homogeneous format while the allosteric ribozyme (RiboReporter) sensor generates a fluorescent signal upon ADP-dependent ribozyme self-cleavage. Both systems perform well when configured for high-throughput screening and have been used to rediscover a known protein kinase inhibitor in a high-throughput screening format.

Introduction

Enzymes represent one of the largest classes of protein targets for pharmaceutical development. High throughput screening (HTS) of compound libraries to identify molecules that inhibit the catalytic activity of specific kinases, helicases, proteases, and other enzymes is a major focus of pharmaceutical industry efforts. Strategies for the detection of enzyme activity in HTS formats that can readily translate to multiple targets have the potential to greatly accelerate therapeutic discovery. Agents such as aptamers that very selectively recognize the common product of an enzyme reaction class but not the corresponding substrate(s) could effectively enable such strategies to the extent that enzyme product recognition can be readily transduced into a detectible signal. Exploiting the ability to select in vitro for and against recognition of product (ADP) and substrate (ATP), respectively, we isolated an aptamer that effectively monitors the catalytic activity of protein kinases. We show that the aptamer and a catalytically active ribozyme (RiboReporter) derived from the aptamer can be configured to generate radiometric and fluorescent readouts, respectively, in HTS formats.

Protein kinases comprise a large family of enzymes that catalyze the transfer of a phosphate group from a nucleoside triphosphate (usually ATP) to a protein substrate, yielding a phosphorylated protein and a nucleoside diphosphate (ADP). The majority of protein kinases fall into either of two classes: those which preferentially phosphorylate a tyrosine residue and those which preferentially phosphorylate a serine and/or threonine residue. More recently, a third class of protein kinases has been described that phosphorylates the imidazole nitrogen on a histidine residue [1]. Notably, over 500 genes containing a kinase catalytic domain have been identified in the human genome, accounting for roughly 1.5% of all human genes [2]. The signal transduction activities of protein kinases are critical for normal functioning of the eukaryotic cell and for its responses to a wide variety of extracellular or environmental stimuli. Aberrant activity of protein kinases is implicated in numerous diseases, ranging from cancer to inflammation and immune disorders [3–8]. Thus, protein kinases represent important targets for discovery of new pharmaceutical agents.

Despite the facts that protein kinases represent an enormous reservoir of targets for small molecule antagonists and that the number of small molecules able to inhibit kinases is also relatively large, there are currently only two FDA-approved small molecule drugs that target protein kinases [4, 9]. These are Gleevec (Novartis) [10, 11], which targets the three kinases Brc-Abl, c-Kit and PDGFR, and Iressa (AstraZeneca) [12, 13], which targets EGFR (HER1) . Since diverse kinases share a common mechanism, specificity among them is very difficult to achieve with small molecule inhibitors. Thus, while many ATP analogs and related compounds that bind to the active site may function as excellent kinase inhibitors, most suffer from toxicities associated with poor target specificity [5]. Since the probability of finding a small molecule inhibitor with the appropriate activity *and* specificity is low, the discovery effort greatly benefits from the development of efficient screening methods that maximize the number of evaluated candidates.

Currently, screens for kinase inhibitors are estimated to represent 10%–20% of the HTS effort in the pharmaceutical industry, and several assay formats have been developed to support these large-scale undertakings [14–16]. Most biochemical assays to detect protein kinase activity monitor phosphorylation of the protein substrate or of a specially engineered peptide surrogate. Traditional enzyme-linked immunosorbent assay (ELISA) formats require custom anti-phosphopeptide-specific antibodies and involve multiple reagent additions and plate washing steps that compromise throughput [17]. More recently, fluorescence polarization [18, 19] and time-resolved fluorescence resonance energy transfer (TR-FRET) [20–24] assays have been developed for protein kinase screens. Nevertheless, like ELISAs, these formats often rely on availability of anti-phosphopeptide-specific antibodies. Several scintillation proximity assay (SPA) formats for HTS of protein kinases have also been reported that use common immobilization formats (e.g., biotin/streptavidin) to capture radiolabeled peptide reaction products on scintillant-containing surfaces [20, 22, 25, 26]. Generally, however, the peptide substrate used in such assay formats must be optimized for each particular kinase and engineered extensively for purposes of detection.

*Correspondence: diener@archemix.com

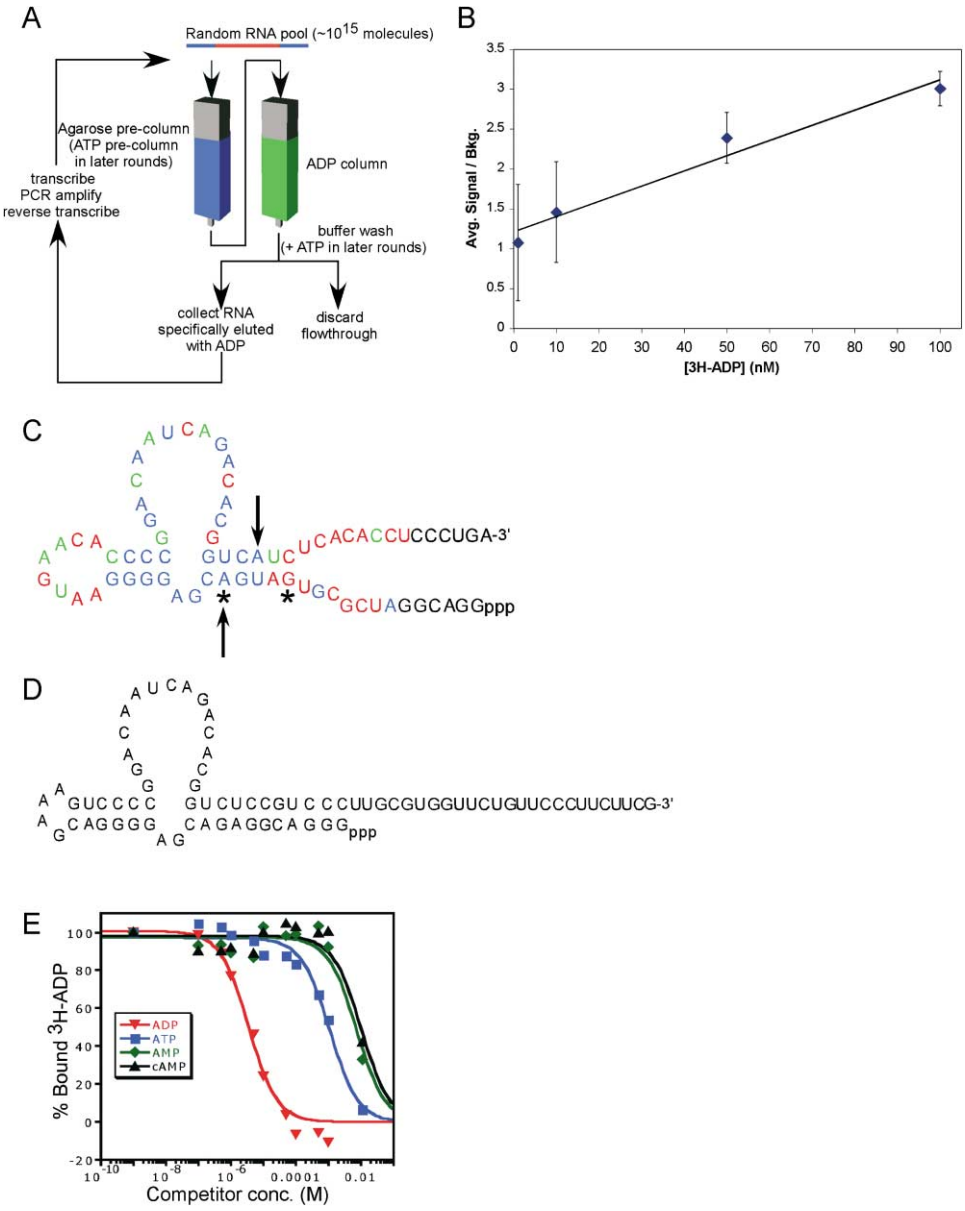

Figure 1. Selection and Initial Characterization of an ADP-Specific Aptamer

(A) Schematic representation of the selection scheme used to generate ADP specific aptamers.

(B) Titration of ^{3}H-ADP against clone F11 from the aptamer selection immobilized in a neutravidin coated scintillation proximity assay (SPA) flash plate via hybridization with a biotinylated capture oligo. Signal over background was calculated by dividing signal with the immobilized best aptamer clone by the signal for immobilized naive pool RNA at the same concentration of ^{3}H-ADP.

(C) Proposed secondary structure of the clone F11 from the original aptamer selection with results from sequence analysis of the doped reselection mapped onto it in color. Red indicates positions that were not conserved, green indicates positions that were moderately conserved, blue indicates positions that were highly conserved, black indicates positions that were held constant during reselection, stars indicate positions where covariation was observed, and arrows indicate the primer boundaries from the original selection.

(D) Sequence and secondary structure of the aptamer sensor used in competition and protein kinase assays. The sequence was designed based upon the results of the reselection, with stabilizing helices flanking the asymmetric bulge region. The sequence was designed with an extended 3′ sequence for use in an oligo capture format in addition to capture by direct 3′-biotinylation.

(E) Competition experiments using the optimized aptamer shown in (D), directly biotinylated at the 3′ end and captured in a neutravidin coated 96-well SPA plate. 1 μM ^{3}H-ADP was added in selection buffer and then competed off with increasing concentrations of unlabeled ADP, ATP, AMP, and cAMP.

Our approach to the establishment of novel protein kinase assay formats relies on detection of ADP rather than the phosphopeptide product of enzymatic activity. The classical detection system couples the generation of ADP to the depletion of the chromophore NADH through the activities of pyruvate kinase and lactate dehydrogenase [27]. While this assay can be configured for HTS, because of its colorimetric readout it typically

Table 1. Relative Affinities of Various Ligands Binding to the ADP Aptamer as Estimated from the IC_{50} in a Competition Experiment with ^{3}H-ADP and Unlabeled Competitor in the SPA Format

Competitor	IC_{50} (μM)	IC_{50} Comp./IC_{50} ADP
ADP	3	1
ATP	1000	300
AMP	7000	2300
cAMP	10000	3300
GDP	2000	700
GTP	4000	1300
GMP	6000	2000
cGMP	13000	4300
Staurosporine[a]	>2000	>700
Iodotubercidin[a]	>1000	>300

[a] For these compounds, solubility became an issue at concentrations greater than 2 and 1 mM, respectively.

has more limited sensitivity. Furthermore, assays that use a secondary enzymatic readout require extensive counter screens (e.g., to control for pyruvate kinase and lactate dehydrogenase-inhibiting compounds, in this particular case). Here, we describe the development of two highly selective RNA-based sensors that can be used to monitor ADP formation in the presence of excess ATP. The first sensor is an ADP-specific aptamer, and the second is an allosteric hammerhead ribozyme (also termed RiboReporter sensor) Both aptamers and RiboReporter sensors are structurally distinctive nucleic acids evolved through in vitro selection to bind their targets with high affinity and specificity [28–39]. Taken together, aptamer and RiboReporter ADP sensor molecules form the basis of efficient and broadly generalizable assay formats for protein kinase activity.

Results and Discussion

ADP Aptamer Selection

Specific recognition of ADP in the presence of excess ATP is conceptually challenging as the two molecules differ by only a single phosphate group. An extensively studied aptamer to ATP, reported almost a decade ago [40], does not discriminate between ATP, ADP, and AMP. In order to build ADP/ATP discrimination into our aptamer, we employed a series of negative selection steps during the SELEX [41–43] process (Figure 1A and Experimental Procedures) in which RNAs that bound to both ATP and ADP were removed from the pool population. After 16 rounds of selection, the aptamer pool was cloned and sequenced, and individual aptamer clones were immobilized via oligonucleotide capture in 96-well neutravidin coated scintillation proximity assay plates. Individual clones were screened on the basis of their ability to both bind to ^{3}H-ADP and to discriminate between ADP and ATP by competition with unlabeled competitor ADP or ATP. As shown (Figure 1B), the best clone, F11, has a lower limit of ^{3}H-ADP detection in the scintillation proximity assay format in the range of 50–100 nM (see Experimental Procedures for details on the SPA assay).

Table 2. Reported K_m^{ATP} Values for Several Protein Kinases

Kinase	Km^{ATP} (μM)	Reference
ERK	140	[44, 45, 50]
MEK1-ED	6	[54]
p38	23	[53]
MAPKAPK2	43	[55]
Rho-kinase II	21	[56, 57]
Cdk2/5	3	[58]
P50/CSK	195	[59–64]
IRK	40	[64, 65]
$pp60^{src}$	80	[67–72]
PKA	7	[62]
IKKα/β	0.13	[77]

In order to better characterize clone F11 from the initial selection, a doped reselection was undertaken using a partially randomized version of the best binding clone sequence as described in Experimental Procedures. After three rounds of reselection, the pool was again cloned and sequenced. Based on both conservation and covariation within the sequence set, we were able to determine the secondary structure of the ADP aptamer and thus design functional minimized constructs for use in assay development (Figures 1C and 1D). Using the SPA competition assay and directly biotinylated minimized aptamer, we estimate the affinity of the ADP aptamer for ADP to be approximately 3 μM. Remarkably, the aptamer discriminates over 300-fold against ATP and other nucleotide derivatives (Figure 1E and Table 1). Specifically, the IC_{50} values for competition of the common kinase inhibitors staurosporine and iodotubercidin (ITU) with ADP for sensor binding are in the low millimolar range (Table 1). Since concentrations of test compounds typically used in HTS assays are in the low- to mid-micromolar range, the level of ADP specificity provided by this sensor will translate into minimal requirements for rescreening caused by test compounds directly competing with ADP for sensor binding.

It is worth noting that the degree of discrimination between ADP and ATP is dependent on the purity of the ATP used. Solutions of purified ATP typically contain up to 1% ADP. As such, the experimentally observed discrimination may represent a lower limit relative to the actual ADP/ATP discrimination of the aptamer. Since K_M values for ATP binding for many protein kinases are in the high-nanomolar to mid-micromolar range (Table 2), kinase assays are typically run at mid-nanomolar to low-micromolar ATP concentrations. In these ranges, given an aptamer binding affinity of ~3 μM, 99% pure ATP will provide 100-fold discrimination and should be more than sufficient to detect ADP produced by kinase activity over background signal.

ADP Aptamer-Based Sensor

The ADP-selective aptamer was configured for use in a scintillation proximity assay (ADP-SPA) that can detect protein kinase activity in a high-throughput setting (Figure 2A). In this scheme, the minimized ADP aptamer (Figure 1D) was immobilized via oligonucleotide capture on a neutravidin-coated 96-well plate embedded with scintillant. When ^{3}H-ATP is used as the substrate in a protein kinase reaction, the ^{3}H-ADP product is captured

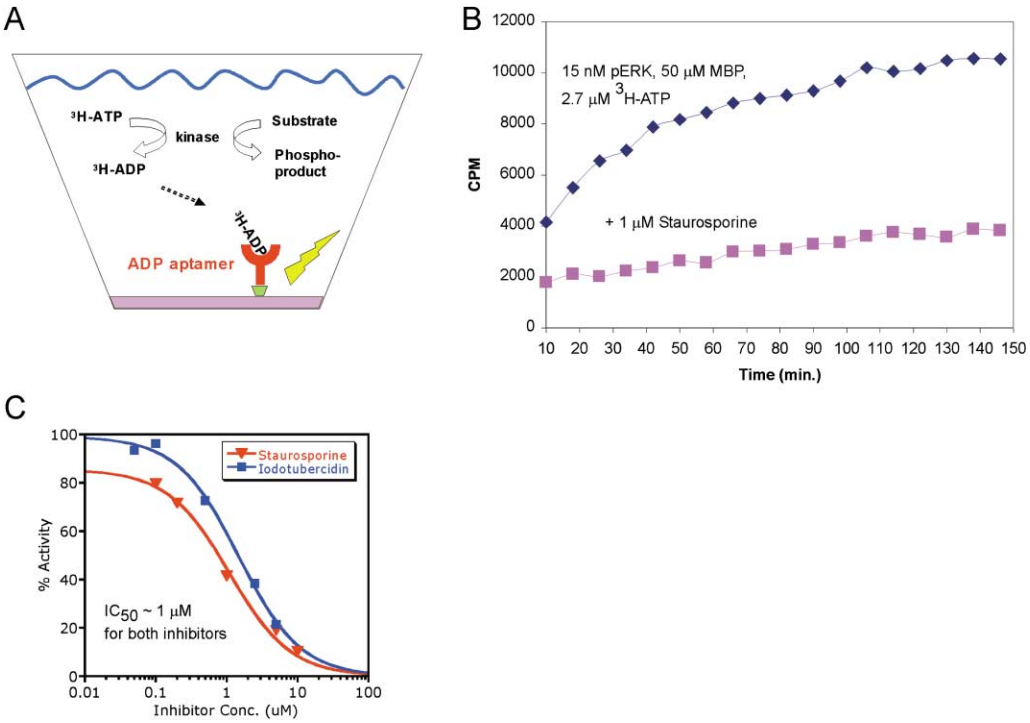

Figure 2. The ADP Aptamer-Based Scintillation Proximity Assay

(A) Schematic representation of the ADP-SPA assay configuration. Optimized aptamer either directly 3′-biotinylated or hybridized via the 3′-sequence tag to a 5′-biotinylated DNA capture oligo is immobilized onto a neutravidin coated scintillation plate. ^{3}H-ATP is used as the substrate for the kinase reaction, yielding ^{3}H-ADP, which is captured by the aptamer on the plate surface, generating a signal.

(B) ADP aptamer-based SPA measuring the activity of the protein kinase pERK2 (15 nM) using MBP (50 μM) and ^{3}H-ATP (2.7 μM) as substrates. Reactions were done in the absence (blue diamonds) or presence (magenta squares) of 1 μM of the kinase inhibitor staurosporine.

(C) Inhibition of protein kinase activity by staurosporine or iodotubercidin in the ADP aptamer SPA. Effect of protein kinase inhibitors was assayed in the presence of 30 nM pERK2, 1.4 μM ^{3}H-ATP, and 10 μM MBP. Activity of pERK2 at various inhibitor concentrations was estimated from initial rates of reaction. Rates in the presence of inhibitor were normalized to the rate of reaction in the absence of any inhibitor. The IC_{50} values determined for both staurosporine and iodotubercidin using the ADP aptamer SPA were ~1 μM. The reported IC_{50} values are 1 μM and 0.9 μM for staurosporine and iodotubercidin inhibition of pERK2, respectively [48].

by the aptamer on the plate surface, generating a signal (Figure 2A). All of the assay components can be added in a single step, and the output can be analyzed either kinetically or as a single point determination. Figure 2B compares the time course of the production of ADP for protein kinase pERK2-catalyzed phosphorylation of myelin basic protein (MBP) [44–46] in the presence and absence of 1 μM staurosporine. As can be seen, the SPA assay provides a direct kinetic profile of the biochemical reaction. Most significantly, IC_{50} values determined for protein kinase inhibitors staurosporine and iodotubercidin acting against pERK2 using the ADP aptamer scintillation proximity assay were in good agreement with their reported values (Figure 2C) [47].

Selection of an ADP-Specific RiboReporter Sensor

In addition to the aptamer-based SPA assay, the minimized ADP aptamer was used to construct a RiboReporter sensor that detects ADP in a background of ATP concomitant with generation of a fluorescent signal. Generation of a RiboReporter sensor was undertaken for two reasons. First, we were interested in generating a detection system that functioned without the use of radioactivity. Second, we were interested in determining whether such a sensor configured in an enzymatic format might have greater sensitivity than the aptamer sensor used in the ADP-SPA format.

Briefly, the ADP aptamer was appended to a hammerhead ribozyme core [48, 49] in two different relative orientations via a connecting stem consisting of eight randomized nucleotides to generate two pools of potential allosteric ribozyme molecules (Figures 3A and 3B). The two pools were used because it was not clear a priori which orientation would yield superior ribozymes. These pools of molecules were subjected to successive rounds of selection in which molecules that were catalytically active in the absence of ADP were selected against, and those that were active in the presence of ADP were amplified and carried forward. After several rounds of selection, the pools were greatly enriched for RNA molecules whose catalytic activity was activated by ADP (Figure 3C). Pools were cloned, sequenced, and screened on the basis of their ADP-dependent reactivity and selectivity against ATP. The sequence and proposed secondary structure of the best clone from the selection is shown (Figure 4A). It is worth noting that the sequence of the best connecting stem was not that of a previously reported communication

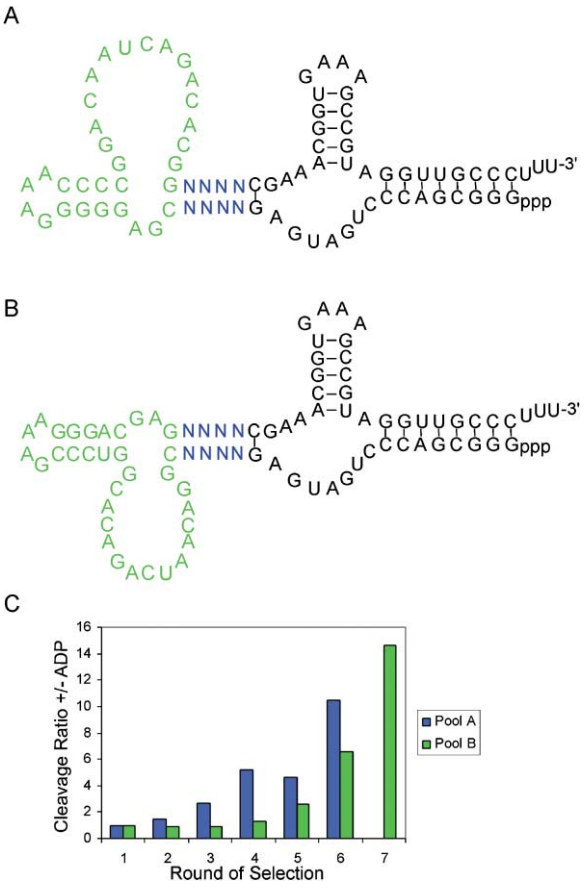

Figure 3. Selection of an ADP-Specific RiboReporter

(A) Proposed secondary structure of ADP RiboReporter sensor pool A.

(B) Proposed secondary structure of riboreporter sensor pool B.

(C) Ratio of riboreporter sensor cleavage in the presence of ADP over the cleavage in the absence of ADP during the course of the selections.

module and furthermore that that particular module did not yield allosteric hammerhead ribozymes with the ADP aptamer in either orientation (data not shown) [35]. Finally, a fluorescence-based signaling system was devised by appending fluorescein to the 3′ terminus of the allosteric ribozyme and hybridizing an oligonucleotide labeled at its 5′ end with Dabcyl immediately proximal to this terminus (Figure 4B and Experimental Procedures). The proximity of the Dabcyl group to the fluorescein quenches fluorescence. Upon binding to ADP, the sensor undergoes self-cleavage at a site near the 3′end, releasing the fluorescently labeled product and generating a fluorescent signal at 535 nanometers.

The ADP RiboReporter sensor is used in a two-step process. In the first step, the protein kinase reaction is run in buffer with the appropriate substrate and ATP in the presence or absence of potential small molecule inhibitors. The protein kinase activity is then quenched, at a specific time such that it is still in the linear region of its reaction profile, by addition of 1 volume of 600 nM RiboReporter in buffer additionally containing 0.1% SDS (see Experimental Procedures). Addition of SDS inhibits protein enzyme activity but not ribozyme activity. The concentration of ADP produced by the kinase reaction is then measured in the second step in a kinetic format in which the rate of production of oligonucleotide cleavage product versus ADP concentration is measured. The rate constant of the self-cleavage reaction increases linearly with ADP concentration, with a lower limit of detection of 1–5 μM ADP (Figure 5A).

The ADP RiboReporter sensor was used to detect pERK2 protein kinase activity in a 96-well format using the synthetic peptide, ERKtide (ATGPLSPGPFGRR) [50], as a substrate. In a pilot screen, 77 test drug-like compounds identified from a chemical library based on Lipinski's "rule of 5" [51] and three positive control wells containing staurosporine were each tested at a final concentration of ~10 μM. As shown (Figure 5B), the ADP RiboReporter sensor unambiguously identified microplate wells containing the staurosporine inhibitor, and its overall performance was acceptable for an unoptimized assay (Z-factor [52] = 0.23). Furthermore, using the ADP RiboReporter in this format, 5–10 μmoles of sensor would be enough to screen a 100,000 compound library.

The ADP aptamer scintillation proximity assay and the

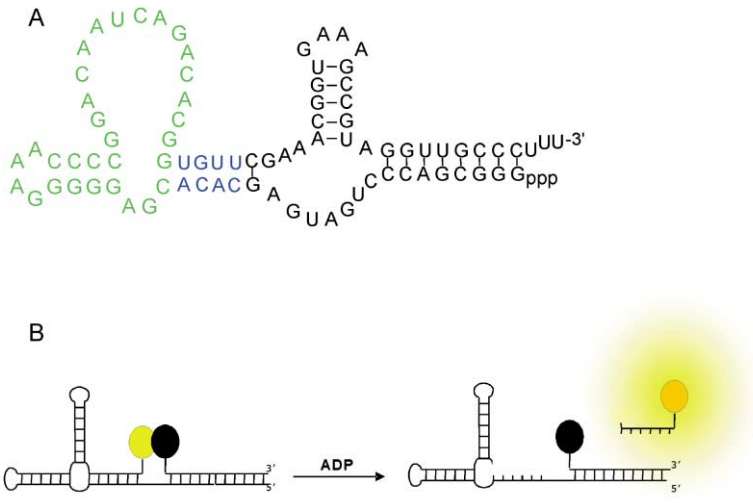

Figure 4. Optimization of the Best ADP-Specific RiboReporter for Fluorescence-Based Detection

(A) Proposed secondary structure of the best ADP-dependent RiboReporter sensor from the two selections. (B) ADP RiboReporter sensor format. The sensor shown in (A) was configured into a fluorescence-based format. Upon binding of ADP, the ribozyme undergoes self-cleavage and releases a short fluorescein-labeled product oligonucleotide, which generates a fluorescent signal at 535 nm upon excitation at 488 nm.

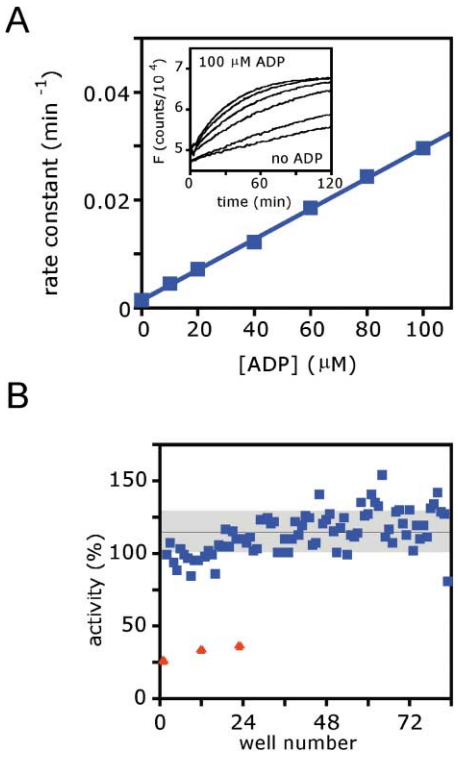

Figure 5. Detection of ADP by the RiboReporter in a High-Throughput Screening Format

(A) The fluorescent signal of the ADP RiboReporter sensor is linearly dependent upon ADP concentration. The RiboReporter sensor (240 nM ribozyme, 1.2 μM quencher oligonucleotide) was incubated with various concentrations of ADP in 50 mM HEPES (pH 8.0), 100 mM NaCl, 10 mM $MgCl_2$, 0.1 mg/ml BSA, 1 mM DTT in a 96-well plate, and the rate of generation of signal was measured using a Fusion fluorescence detector. The initial reaction rates are plotted versus [ADP]. The inset shows the raw fluorescence emission signal at 535 nanometers versus time.

(B) ADP RiboReporter sensor performance in a pilot HTS. 25 nM activated ERK was incubated with 100 μM ATP and 100 μM ERKtide in 50 mM HEPES (pH 8.0), 100 mM NaCl, 10 mM $MgCl_2$, 0.1 mg/ml BSA, 1 mM DTT for 30 min at 25°C in the presence of 10 μM test compound. Reactions were quenched by the addition of 0.1% SDS in reaction buffer plus 600 nM sensor. The initial rates of fluorescence signal generation at 535 nanometers were measured. Results are reported as percentage of activity in the absence of test compound. The shaded area indicates a single standard deviation from the mean observed percent activity. Data points shown in red triangles represent wells containing staurosporine.

ADP RiboReporter sensor provide two novel formats highly suitable for universal detection of protein kinase enzymatic activity. Both assay formats can be adapted for both low- and high-throughput applications. The detection limits for kinase assays using ADP-SPA and RiboReporter sensor are approximately 50–100 nM and 1–5 μM ADP, respectively. While we may have hoped that the RiboReporter sensor would be more sensitive than the aptamer alone, the factors that determine the sensitivity of an allosteric ribozyme are complex. Sensitivity of the aptamer is only dependent on the affinity for the ligand and the detection scheme, while sensitivity of the RiboReporter depends on multiple factors, including the ratio of the rate constants $k_{active}/k_{inactive}$ as well as the affinity of the sensor for the target ligand and the detection scheme [76]. Thus, further selection or doped reselection would be necessary to improve the sensitivity of the current RiboReporter sensor.

Ultimately, these detection limits define subsets of protein kinases that may be assayed using this generation of sensors. The ADP aptamer scintillation proximity assay is appropriate for protein kinases with K_m^{ATP} values in the low-micromolar range, while the ADP RiboReporter sensor is suitable for protein kinases with K_m^{ATP} values in the mid-micromolar range. These reported K_m^{ATP} values [45, 46, 50, 53–75, 77], taken together, cover a substantial range of the spectrum of kinases (Table 2). Continued selection and optimization of an ADP aptamer and/or RiboReporter sensor with an approximate 10-fold increase in affinity for ADP is expected to enable activity assays for nearly every known protein kinase using a single biochemical format. Furthermore, while the detection limit of the RiboReporter sensor is higher than that of the original ADP-SPA, the RiboReporter sensor still retains the specificity of the aptamer and is functional in a nonradioactive format.

Significance

As currently configured, each of our assay formats has certain strengths relative to the other. The aptamer SPA assay offers the advantage of a single-step reaction that can be monitored in real time, providing a direct kinetic measurement of each individual reaction in the screen. While the RiboReporter sensor requires a two-step process, it offers the advantage of a nonradioactive, fluorescence-based readout. However, in both cases, the exquisite selectivity demonstrated by the sensors against ATP, ATP analogs, and nucleotides in general suggests that candidate drug compounds and other components of kinase reactions used in HTS are unlikely to interfere with the detection of ADP. Therefore, unlike traditional enzymatic formats for ADP detection, minimal rescreening of potential lead compounds will be required. Together, the combination of the selectivity and the universality of these sensors represents a significant step forward in the processes of identification and development of small molecule inhibitors of protein kinases as therapeutics.

Experimental Procedures

Synthesis of Primers and Pools

Primers were synthesized either at Integrated DNA Technologies (IDT) or internally on an Expedite 8909 DNA synthesizer using standard methods. The names and sequences of the primers used in various experiments described below are as follows: STC.12.143.A, 5′-TAATACGACTCACTATAGGGCGACCCTGATGAG-3′; STC.12.143.B, 5′-AAAGGGCAACCTACGGCTTTCACCGTTTC-3′; JD.18.25.B, 5′-TAATACGACTCACTATAGGACGGATCGCGTGATGA-3′; JD.18.25.C, 5′-TCAGGGAGGTGTGTGAGAT-3′; JD.18.122.A, 5′-CGAAGAAGGGAACAGAACCACGCAAGGTCAGGGAGGTGTGTGAGAT-3′; JD.18.155.U, 5′-TAATACGACTCACTATAGGACCTGGCTTGGACGG-3′; JD.18.155.V, 5′-AGTCCCGAGCACTTCAGGG-3′; JD.37.98.B, 5′-TAATACGACTCACTATAGGGACGGAGACGAGGG-3′; JD.37.98.C, 5′-CGAAGAAGGGAACAGAACC-3′; MK.08.112A, 5′-biotin-CGAAGAAGGGAACAGAACCACGCAA-3′; MK.08.130.B, 5′-TAATACGACTCACTATAGGATGTCCAGTCGCTTGCAATGCCCTTTTAGACCCTGATGAG-3′,

MK.08.66.B, 5′-AGACCTACGGCTTTCACCGTTTCG-3′; MK.08.87.B, 5′-Dabcyl-TGGGCATTGCAAGCGACTGGACATCC-3′.

The DNA templates for the four pools and the minimized ADP aptamer were prepared on an ABI Expedite 8909 DNA synthesizer using standard methods.

The RNA pools were prepared via run-off transcription using T7 RNA polymerase: JD18.25.A, 5′-GGACGGAUCGCGUGAUGA–N_{40}-AUCUCACACACCUCCCUGA-3′; JD.18.155.W, 5′-AGTCCCGAGC ACTTCAGGG **AGGTGTGTGAGATGACCGTGTCTGATTGTCCGGG GTGTTCATTCCCCTCGTCATCACGCGAT** CCGTCCAAGCCAGG TCC TA TAGTGAGTCGTATTA-3′. Nucleotides shown in bold were incorporated on the DNA synthesizer at 85% WT and 5% each of the other three possible nucleotides. JD.37.98.A, 5′-GGGACGGAGAC GAGGGGACGAAAGTCCCCGGACAATCAGACACGGTCTCCGTCC CTTGCGTGGTTCTGTTCCCTTCTTC-3′; JD.37.71.A, 5′-GGGCGAC CCUGAUGAGNNNNCGAGGGGGAAACCCGGACAAUCAGACACGGN NNNCGAAACGGUGAAAGCCGUAGGUUGCCCUUU-3′; JD.37.71.B, 5′-GGGCGACCCUGAUGAGNNNNCGGACAAUCAGACACGGUCCC GAAAGGGACGAGNNNNCGAAACGGUGAAAGCCGUAGGUUGCCC UUU-3′.

DNA templates containing the T7 promoter sequence (0.5 μM) were incubated with 2.5 units/μl T7 RNA polymerase overnight at 37°C in transcription buffer (40 mM Tris [pH 7.8], 25 mM $MgCl_2$, 1 mM spermidine, 0.1% Triton X-100, 5 mM each NTP, 40 mM DTT) as described [73]. Reactions were quenched with 50 mM EDTA, ethanol precipitated, and then purified on a denaturing polyacrylamide gels (8 M urea, 10% acrylamide; 19:1 acrylamide:bisacrylamide). Prior to use, the naive pool RNA was treated with RQ1 DNase (Promega) under the prescribed conditions to remove residual template DNA.

In Vitro Selection of an ADP-Specific Aptamer

C-8-linked ADP agarose resin (Sigma) loaded at 1.6 μmole/ml slurry was used as the selection substrate. Two types of pre-column were used. In rounds 1–9, pool RNA was passed over an agarose column derivatized with adipic acid dihydrazide (AAD-agarose) to remove matrix binders. In rounds 10–16, molecules lacking the ability to differentiate between ATP and ADP were removed by passing them over an agarose column derivatized with C-8-linked ATP (5 μmole/l; Sigma).

Both the pre-column (AAD-agarose or ATP-agarose) and the substrate (ADP-agarose) resins (100–400 μl, depending on the round) were added to disposable 1 cm columns and equilibrated with selection buffer (50 mM HEPES [pH 7.4], 25 mM $MgCl_2$, 150 mM NaCl) containing 10 μg/ml tRNA. The pre-column was inserted directly into the top of the ADP column to allow pool RNA to flow directly from one column to the next. Trace ^{32}P-labeled pool RNA (round 1, 7 nmole; subsequent rounds, 100–500 pmole) in 200–300 μl selection buffer was added to the resin and incubated for 5 min. The resin was washed between 12 and 35 times with 200–300 μl of selection buffer (in rounds 6–16, washes with selection buffer containing 4 mM ATP were included). After the third wash, the pre-column was removed and the wash solutions were added directly to the ADP column. Throughout, each wash fraction was incubated on the resin for 2–3 min. To elute specifically bound RNA molecules, the resin was treated with from 4–8 aliquots of selection buffer containing 4 mM ADP. All fractions were quantified using the Bioscan QC 2000 counter (Bioscan, Inc., Washington, D.C.). The elution fractions were combined, and 25 mM EDTA, 40 μg glycogen, and 1 volume of isopropanol were added to precipitate the pool RNA. The recovered RNA was hybridized to JD.18.25.C and reverse transcribed (Superscript II, Invitrogen), then amplified by PCR (Taq polymerase, Invitrogen) using the primers JD.18.25.B and JD.18.25.C according to recommended standard protocols. Pool RNA for subsequent rounds of selection were transcribed as described in the pool preparation section.

Clonal Analysis and Sequencing

After the sixteenth round of selection, the amplified selected pool PCR product was cloned using the TOPO-TA cloning kit from Invitrogen following standard protocols. Agar plates were sent to Lark Technologies (Houston, TX) for growth, DNA purification, and sequencing. Individual aptamer clones were PCR amplified from purified plasmid DNA using the primers JD.18.25.B and JD.18.122A. The primer JD.18.122A appends a sequence tag to the 3′ end of each clone that is complementary to the biotinylated capture probe, MK.08.112A. Clones were the transcribed as described above. Using neutravidin-coated SPA flash plates (NEN) and prebound capture probe (~40 pmol), MK.08.112A, 5 μl of individual crude clone transcriptions in 25 μl of PBS was captured in the plates. Unbound RNA was removed with three washes with 200 μl of PBS. Plates were then patted dry on a paper towel. Treated wells were incubated with 30 μl of 1 μM ^{3}H-ADP in 1× selection buffer for 30 s with shaking at 650 rpm and then assessed for ADP-mediated signal by quantification on a TopCount NXT microplate and luminescence counter (Packard). The clone that gave the highest signal over background and whose signal was least attenuated by the addition of excess ATP in 1× selection buffer was identified as the "best clone." Background was estimated based on the signal generated by surface immobilization of unselected naive pool RNA under the same conditions. The best clone, clone F11, was then used to estimate the lower limit of detection of ^{3}H-ADP in the SPA format by titrating the concentration of ^{3}H-ADP against both immobilized clone F11 and naive pool in parallel (Figure 1B).

Doped Reselection

JD.18.155W pool template was transcribed and purified as described above. Approximately 170 pmol of purified pool RNA was incubated in 1× reselection buffer (1% DMSO, 100 mM NaCl, 10 mM $MgCl_2$, 10 mM $MnCl_2$, 1 mM DTT, 50 mM HEPES [pH 7.1]) plus 10 mg/ml tRNA. Pool RNA was applied to an ATP agarose precolumn as described above with the flow through passing directly onto the ADP agarose column. The ADP column was washed 15–20 times as described above with both reselection buffer and reselection buffer containing 4 mM ATP. Bound RNA was eluted with 5–8 200 μl of reselection buffer containing 4 mM ADP. Eluted RNA was precipitated with ethanol and amplified by reverse transcription and PCR amplification as described above using the primers JD.18.155U and JD.18.155V. After three rounds of reselection, the pool was cloned and sequenced as described above. Sequences were aligned and analyzed for conservation and covariation using the programs Bioedit and Clustal.

Measurement of Dissociation Constants for Aptamer:Ligand Complexes

Preparation of Biotin-Labeled ADP Aptamer

The minimized aptamer was transcribed off of a PCR product made by amplification of the JD.37.98A DNA template with the primers JD.37.98B and JD.87.98C. The minimized ADP aptamer was purified on denaturing PAGE and then biotinylated at the 3′ end using a two-step process. RNA (~10 μM) was incubated with 10 mM sodium metaperiodate and 75 mM sodium acetate (pH 5.4) for 1 hr on ice in the dark. The oxidized RNA was desalted with a Centrisep gel filtration column (Princeton Separations), then resuspended at a concentration of approximately 4 μM in a reaction mix containing 150 mM sodium acetate (pH 5.4) and 2 mM biotin thiosemicarbazide. The mixture was reacted for 2 hr at room temperature with shaking at 500 rpm. The RNA was purified using a Centrisep gel filtration column that had been pre-equilibrated with water. Biotinylated aptamer (5 pmole/well) was immobilized to streptavidin flash plates (NEN) by incubation in 25 μl PBS plus 0.05% tRNA, 0.025% Tween 20 with shaking at 650 rpm for 30 min. Unbound biotinylated aptamer probe was rinsed from the plate with three 1× PBS washes and dried.

To determine the dissociation constants for ADP and its analogs, treated wells were incubated with 30 μl of 1 μM ^{3}H-ADP in 1× reselection buffer for 30 s with shaking at 650 rpm and then assessed for ADP-mediated signal by quantification on a TopCount NXT microplate and luminescence counter (Packard). Thereafter, 1 μl of each test compound was added to the appropriate wells, and the plate was shaken at 650 rpm for 30 s prior to recounting. Titration of each test compound was continued with subsequent 1 μl additions up to between 1 and 10 mM final concentrations (depending on solubility and ability to compete with ADP). Affinities of various

ligands for the aptamer were estimated from the IC_{50} of the competitive binding curves by fitting the data to the following equation:

$$\% \text{ bound}_{3H\text{-}ADP} = \% \text{ bound}_{3H\text{-}ADP0}/(1 + ([\text{competitor}]/IC_{50comp.})).$$

ADP Aptamer-Based Assay for Kinase Activity

The assay for pERK2 kinase activity was configured in 96-well SPA format [26]. The ADP aptamer was appended with a tag at the 3′ end to allow the aptamer to be immobilized onto the surface of an NEN streptavidin coated flash plate via base pairing with a biotinylated DNA capture oligo MK08.112A. Flash plates (NEN) were prepared by incubating the individual wells with 40 pmol of MK08.112A biotinylated capture probe in 22 μl of PBS plus 0.05% tRNA, 0.025% Tween-20 with shaking at 650 rpm for 15 min. Excess capture probe was removed from the wells by washing with PBS three times, inverting plates with force sufficient to remove liquid, and blotting them dry on paper towels. Transcription reactions of the minimized ADP aptamer containing capture probe sequence (5 μl, ~5 pmole) in 25 μl 1× PBS were incubated in designated wells with shaking at 650 rpm for 30 min. Excess aptamer was removed by washing with 1× PBS three times and blotting as described above.

Conversion of ^{3}H-ATP to ^{3}H-ADP as a result of phosphorylation of MBP (Sigma) by pERK was measured by capture of ^{3}H-ADP onto the plate surface. pERK was generated from ERK2 by activation with constitutively active MEK-1 mutant (MEK-DD) [74, 75] and separated from unphosphorylated ERK2 using a MonoQ column. Flash plates containing individual reaction mixtures comprised of 40 nM pERK, 5 μM MBP, and 1.35 μM ^{3}H-ATP in 50 μl buffer (1% DMSO, 100 mM NaCl, 10 mM $MgCl_2$, 10 mM $MnCl_2$, 1 mM DTT, 50 mM HEPES [pH 7.1]) were incubated in a TopCount plate reader at room temperature. Each well was counted approximately every 5 min. Reaction rates were estimated from the slope of the initial phase of the reactions.

The known kinase inhibitors staurosporine and iodotubercidin (ITU) were purchased from Sigma and Alexis, respectively.

In Vitro Selection of an ADP-Specific RiboReporter Sensor

A general strategy for the selection of hammerhead-based RiboReporter sensors has been described [34]. Briefly, the pools (JD.37.71.A, JD.37.71.B) were subjected to successive cycles of negative and positive selection. For all rounds but the first, the process began with the negative selection step. Pool RNA ~3 μM was incubated for a fixed period of time at room temperature in selection buffer (1% DMSO, 0.01% bovine γ-globulin, 100 mM NaCl, 10 mM $MgCl_2$, 10 mM $MnCl_2$, 1 mM DTT, 50 mM HEPES [pH 7.1]). The reaction was quenched by the addition of 50 mM EDTA and then precipitated by the addition of 300 mM NaOAc and 1.5 reaction volumes of 2:1 isopropanol:ethanol. After precipitation, the pool RNA was subjected to a denaturation step. In rounds 1–4, chemical denaturation was used. The pool pellet was resuspended in 90 μl H_2O, followed by the addition of 10 ul 100 mM NaOH. The tube was lightly vortexed, then 12 μl NaOAc was added, and the material was isopropanol:ethanol precipitated. In rounds 5 and 6, after quenching the reaction with EDTA, the sample was heated at 90°C for 2 min, followed by brief cooling on ice, addition of 300 mM NaOAc, and isopropanol:ethanol precipitation. During each negative selection step, two denaturation steps were performed. After the final negative incubation step, samples were precipitated, and cleaved and uncleaved pool molecules were separated on a 10% denaturing polyacrylamide gel. Uncleaved molecules were eluted from the gel and precipitated. Eighty percent of the RNA was carried forward into the positive selection step where it was incubated for a fixed period of time in selection buffer plus 1 mM ADP. Reactions were quenched with 50 mM EDTA and precipitated with 300 mM NaOAc and isopropanol:ethanol. Cleaved pool molecules were purified using a 10% denaturing gel followed by elution and precipitation. The recovered RNA was hybridized to STC.12.143.B and reverse transcribed (ThermoScript RT, Invitrogen), then amplified by PCR (Taq polymerase, Invitrogen) using the primers STC.12.143.A and STC.12.143.B according to recommended standard protocols. Pool RNA for the following round of selection was transcribed as described in the pool preparation section.

ADP RiboReporter Sensor-Based Assay for Kinase Activity

Preparation of Fluorescein-Labeled RiboReporter Sensor

The template for the ADP RiboReporter sensor (SCK.46.58.A3) was amplified by PCR using the primers MK.08.130.B and MK.08.66.B by standard protocols (Taq polymerase, Invitrogen). The template was used to program in vitro transcription using the protocol described above. The transcripts were desalted using a Nap5 gel filtration column (Pharmacia), then quantitated by OD_{260}. Next, the RNA (50 μM) was incubated with 10 mM sodium metaperiodate and 300 mM sodium acetate (pH 5.4) for 1 hr on ice in the dark. Following precipitation with 200 μl isopropanol, the 3′-oxidized RNA was resuspended at a concentration of approximately 40 μM in a reaction mix containing 250 mM sodium acetate (pH 5.4) and 3 mM fluorescein thiosemicarbazide (7% DMSO final). The mixture was reacted for 2 hr at room temperature, after which the labeled nucleic acid was precipitated, purified by gel-electrophoresis on a 10% denaturing polyacrylamide gel, and resuspended in H_2O to a final concentration of 12 μM.

To generate the RiboReporter sensor, the fluorescein-labeled transcript was annealed to the quenching oligonucleotide MK.08.87.B in 10 mM Tris (pH 7.4), 50 mM NaCl.

pERK kinase activity was measured by combining 25 nM activated pERK with 100 μM ATP and 100 μM ERKtide in 50 mM HEPES (pH 8.0), 100 mM NaCl, 10 mM $MgCl_2$, 0.1 mg/ml BSA, 1 mM DTT for 30 min at 25°C in the presence or absence of 10 μM test compound in 50 μl. Reactions were quenched by the addition of an equal volume of 0.1% SDS in reaction buffer plus 600 nM RiboReporter sensor. The fluorescence signal at 535 nanometers versus time was monitored on a Fusion α-FP plate reader. Relative kinase activity was estimated based on the initial rate of the cleavage reaction of the RiboReporter sensor, which is determined by the concentration of ADP in the solution.

Acknowledgments

The authors would like to acknowledge Dr. Judith Healy for her extensive help and advice during the preparation of this manuscript.

Received: November 21, 2003
Revised: January 9, 2004
Accepted: January 12, 2004
Published: April 16, 2004

References

1. Saito, H. (2001). Histidine phosphorylation and two-component signaling in eukaryotic cells. Chem. Rev. *101*, 2497–2509.
2. Manning, G., Whyte, D.B., Martinez, R., Hunter, T., and Sudarsanam, S. (2002). The protein kinase complement of the human genome. Science *298*, 1912–1934.
3. Moelling, K., Strack, B., and Radziwill, G. (1996). Signal transduction as target of gene therapy. Recent Results Cancer Res. *142*, 63–71.
4. Fabbro, D., and Garcia-Echeverria, C. (2002). Targeting protein kinases in cancer therapy. Curr. Opin. Drug Discov. Dev. *5*, 701–712.
5. Orchard, S. (2002). Kinases as targets: prospects for chronic therapy. Curr. Opin. Drug Discov. Dev. *5*, 713–717.
6. Chen, G., and Goeddel, D.V. (2002). TNF-R1 signaling: a beautiful pathway. Science *296*, 1634–1635.
7. Alton, G., Schwamborn, K., Satoh, Y., and Westwick, J.K. (2002). Therapeutic modulation of inflammatory gene transcription by kinase inhibitors. Expert Opin. Biol. Ther. *2*, 621–632.
8. Chen, W., and Wahl, S.M. (2002). TGF-beta: receptors, signaling pathways and autoimmunity. Curr. Dir. Autoimmun. *5*, 62–91.
9. Shawver, L.K., Slamon, D., and Ullrich, A. (2002). Smart drugs: tyrosine kinase inhibitors in cancer therapy. Cancer Cell *1*, 117–123.
10. Buchdunger, E., O'Reilly, T., and Wood, J. (2002). Pharmacology of imatinib (STI571). Eur. J. Cancer *38* (*Suppl 5*), S28–S36.
11. McGary, E.C., Weber, K., Mills, L., Doucet, M., Lewis, V., Lev, D.C., Fidler, I.J., and Bar-Eli, M. (2002). Inhibition of platelet-derived growth factor-mediated proliferation of osteosarcoma

cells by the novel tyrosine kinase inhibitor STI571. Clin. Cancer Res. *8*, 3584–3591.
12. Ranson, M., Hammond, L.A., Ferry, D., Kris, M., Tullo, A., Murray, P.I., Miller, V., Averbuch, S., Ochs, J., Morris, C., et al. (2002). ZD1839, a selective oral epidermal growth factor receptor-tyrosine kinase inhibitor, is well tolerated and active in patients with solid, malignant tumors: results of a phase I trial. J. Clin. Oncol. *20*, 2240–2250.
13. Ciardiello, F., Bianco, R., Damiano, V., Fontanini, G., Caputo, R., Pomatico, G., De Placido, S., Bianco, A.R., Mendelsohn, J., and Tortora, G. (2000). Antiangiogenic and antitumor activity of anti-epidermal growth factor receptor C225 monoclonal antibody in combination with vascular endothelial growth factor antisense oligonucleotide in human GEO colon cancer cells. Clin. Cancer Res. *6*, 3739–3747.
14. Schlessinger, J. (2002). A solid base for assaying protein kinase activity. Nat. Biotechnol. *20*, 232–233.
15. Zaman, G.J., Garritsen, A., de Boer, T., and van Boeckel, C.A. (2003). Fluorescence assays for high-throughput screening of protein kinases. Comb. Chem. High Throughput Screen. *6*, 313–320.
16. Mallari, R., Swearingen, E., Liu, W., Ow, A., Young, S.W., and Huang, S.G. (2003). A generic high-throughput screening assay for kinases: protein kinase a as an example. J. Biomol. Screen. *8*, 198–204.
17. Ross, H., Armstrong, C.G., and Cohen, P. (2002). A non-radioactive method for the assay of many serine/threonine-specific protein kinases. Biochem. J. *366*, 977–981.
18. Parker, G.J., Law, T.L., Lenoch, F.J., and Bolger, R.E. (2000). Development of high throughput screening assays using fluorescence polarization: nuclear receptor-ligand-binding and kinase/phosphatase assays. J. Biomol. Screen. *5*, 77–88.
19. Seethala, R., and Menzel, R. (1998). A fluorescence polarization competition immunoassay for tyrosine kinases. Anal. Biochem. *255*, 257–262.
20. Sills, M.A., Weiss, D., Pham, Q., Schweitzer, R., Wu, X., and Wu, J.J. (2002). Comparison of assay technologies for a tyrosine kinase assay generates different results in high throughput screening. J. Biomol. Screen. *7*, 191–214.
21. Bader, B., Butt, E., Palmetshofer, A., Walter, U., Jarchau, T., and Drueckes, P. (2001). A cGMP-dependent protein kinase assay for high throughput screening based on time-resolved fluorescence resonance energy transfer. J. Biomol. Screen. *6*, 255–264.
22. Park, Y.W., Cummings, R.T., Wu, L., Zheng, S., Cameron, P.M., Woods, A., Zaller, D.M., Marcy, A.I., and Hermes, J.D. (1999). Homogeneous proximity tyrosine kinase assays: scintillation proximity assay versus homogeneous time-resolved fluorescence. Anal. Biochem. *269*, 94–104.
23. Braunwalder, A.F., Yarwood, D.R., Sills, M.A., and Lipson, K.E. (1996). Measurement of the protein tyrosine kinase activity of c-src using time-resolved fluorometry of europium chelates. Anal. Biochem. *238*, 159–164.
24. Rodems, S.M., et al. (2002). A FRET-based assay platform for ultra-high density drug screening of protein kinases and phosphatases. Assay Drug Dev. Technol. *1*, 9–19.
25. Beveridge, M., Park, Y.W., Hermes, J., Marenghi, A., Brophy, G., and Santos, A. (2000). Detection of p56(lck) kinase activity using scintillation proximity assay in 384-well format and imaging proximity assay in 384- and 1536-well format. J. Biomol. Screen. *5*, 205–212.
26. McDonald, O.B., Chen, W.J., Ellis, B., Hoffman, C., Overton, L., Rink, M., Smith, A., Marshall, C.J., and Wood, E.R. (1999). A scintillation proximity assay for the Raf/MEK/ERK kinase cascade: high-throughput screening and identification of selective enzyme inhibitors. Anal. Biochem. *268*, 318–329.
27. Jenkins, W.T. (1991). The pyruvate kinase-coupled assay for ATPases: a critical analysis. Anal. Biochem. *194*, 136–139.
28. Bacher, J.M., and Ellington, A.D. (1998). Nucleic acid selection as a tool for drug discovery. Drug Discov. Today *3*, 265–273.
29. Ellington, A.D., and Conrad, R. (1995). Aptamers as potential nucleic acid pharmaceuticals. Biotechnol. Annu. Rev. *1*, 185–214.
30. Osborne, S.E., Matsumura, I., and Ellington, A.D. (1997). Aptamers as therapeutic and diagnostic reagents: problems and prospects. Curr. Opin. Chem. Biol. *1*, 5–9.
31. Carmi, N., Shultz, L.A., and Breaker, R.R. (1996). In vitro selection of self-cleaving DNAs. Chem. Biol. *3*, 1039–1046.
32. Breaker, R.R. (1997). In vitro selection of catalytic polynucleotides. Chem. Rev. *97*, 371–390.
33. Koizumi, M., and Breaker, R.R. (2000). Molecular recognition of cAMP by an RNA aptamer. Biochemistry *39*, 8983–8992.
34. Koizumi, M., Soukup, G.A., Kerr, J.N., and Breaker, R.R. (1999). Allosteric selection of ribozymes that respond to the second messengers cGMP and cAMP. Nat. Struct. Biol. *6*, 1062–1071.
35. Soukup, G.A., and Breaker, R.R. (1999). Engineering precision RNA molecular switches. Proc. Natl. Acad. Sci. USA *96*, 3584–3589.
36. Hesselberth, J., Robertson, M.P., Jhaveri, S., and Ellington, A.D. (2000). In vitro selection of nucleic acids for diagnostic applications. J. Biotechnol. *74*, 15–25.
37. Marshall, K.A., and Ellington, A.D. (2000). In vitro selection of RNA aptamers. Methods Enzymol. *318*, 193–214.
38. Robertson, M.P., and Ellington, A.D. (1999). In vitro selection of an allosteric ribozyme that transduces analytes to amplicons. Nat. Biotechnol. *17*, 62–66.
39. Kurz, M., and Breaker, R.R. In vitro selection of nucleic acid enzymes. (1999). Curr. Top. Microbiol. Immunol. *243*, 137–158.
40. Sassanfar, M., and Szostak, J.W. (1993). An RNA motif that binds ATP. Nature *364*, 550–553.
41. Fitzwater, T., and Polisky, B. (1996). A SELEX primer. Methods Enzymol. *267*, 275–301.
42. Gold, L. (1995). The SELEX process: a surprising source of therapeutic and diagnostic compounds. Harvey Lect. *91*, 47–57.
43. Tuerk, C., and MacDougal-Waugh, S. (1993). In vitro evolution of functional nucleic acids: high-affinity RNA ligands of HIV-1 proteins. Gene *137*, 33–39.
44. Prowse, C.N., Deal, M.S., and Lew, J. (2001). The complete pathway for catalytic activation of the mitogen-activated protein kinase, ERK2. J. Biol. Chem. *276*, 40817–40823.
45. Prowse, C.N., and Lew, J. (2001). Mechanism of activation of ERK2 by dual phosphorylation. J. Biol. Chem. *276*, 99–103.
46. Robbins, D.J., Zhen, E., Owaki, H., Vanderbilt, C.A., Ebert, D., Geppert, T.D., and Cobb, M.H. (1993). Regulation and properties of extracellular signal-regulated protein kinases 1 and 2 in vitro. J. Biol. Chem. *268*, 5097–5106.
47. English, J.M., and Cobb, M.H. (2002). Pharmacological inhibitors of MAPK pathways. Trends Pharmacol. Sci. *23*, 40–45.
48. Tang, J., and Breaker, R.R. (1998). Mechanism for allosteric inhibition of an ATP-sensitive ribozyme. Nucleic Acids Res. *26*, 4214–4221.
49. Forster, A.C., and Symons, R.H. (1987). Self-cleavage of plus and minus RNAs of a virusoid and a structural model for the active sites. Cell *49*, 211–220.
50. Prowse, C.N., Hagopian, J.C., Cobb, M.H., Ahn, N.G., and Lew, J. (2000). Catalytic reaction pathway for the mitogen-activated protein kinase ERK2. Biochemistry *39*, 14002.
51. Lipinski, C.A., Lombardo, F., Dominy, B.W., and Feeney, P.J. (1997). Experimental and computational approaches to estimate solubility and permeability in drug discovery and development settings. Adv. Drug Deliv. Rev. *46*, 3–26.
52. Zhang, J.H., Chung, T.D., and Oldenburg, K.R. (1999). A simple statistical parameter for use in evaluation and validation of high throughput screening assays. J. Biomol. Screen. *4*, 67–73.
53. Waas, W.F., Lo, H.H., and Dalby, K.N. (2001). The kinetic mechanism of the dual phosphorylation of the ATF2 transcription factor by p38 mitogen-activated protein (MAP) kinase alpha. Implications for signal/response profiles of MAP kinase pathways. J. Biol. Chem. *276*, 5676–5684.
54. Horiuchi, K.Y., Scherle, P.A., Trzaskos, J.M., and Copeland, R.A. (1998). Competitive inhibition of MAP kinase activation by a peptide representing the alpha C helix of ERK. Biochemistry *37*, 8879–8885.
55. Schindler, J.F., Godbey, A., Hood, W.F., Bolten, S.L., Broadus, R.M., Kasten, T.P., Cassely, A.J., Hirsch, J.L., Merwood, M.A., Nagy, M.A., et al. (2002). Examination of the kinetic mechanism of mitogen-activated protein kinase activated protein kinase-2. Biochim. Biophys. Acta *1598*, 88–97.

56. Trauger, J.W., Lin, F.F., Turner, M.S., Stephens, J., and Lo-Grasso, P.V. (2002). Kinetic mechanism for human Rho-Kinase II (ROCK-II). Biochemistry *41*, 8948–8953.
57. Turner, M.S., Fen-Fen-Lin, Trauger, J.W., Stephens, J., and Lo-Grasso, P. (2002). Characterization and purification of truncated human Rho-kinase II expressed in Sf-21 cells. Arch. Biochem. Biophys. *405*, 3–20.
58. Clare, P.M., Poorman, R.A., Kelley, L.C., Watenpaugh, K.D., Bannow, C.A., and Leach, K.L. (2001). The cyclin-dependent kinases cdk2 and cdk5 act by a random, anticooperative kinetic mechanism. J. Biol. Chem. *276*, 48292–48299.
59. Cole, P.A., Burn, P., Takacs, B., and Walsh, C.T. (1994). Evaluation of the catalytic mechanism of recombinant human Csk (C-terminal Src kinase) using nucleotide analogs and viscosity effects. J. Biol. Chem. *269*, 30880–30887.
60. Cole, P.A., Grace, M.R., Phillips, R.S., Burn, P., and Walsh, C.T. (1995). The role of the catalytic base in the protein tyrosine kinase Csk. J. Biol. Chem. *270*, 22105–22108.
61. Grace, M.R., Walsh, C.T., and Cole, P.A. (1997). Divalent ion effects and insights into the catalytic mechanism of protein tyrosine kinase Csk. Biochemistry *36*, 1874–1881.
62. Shaffer, J., and Adams, J.A. (1999). An ATP-linked structural change in protein kinase A precedes phosphoryl transfer under physiological magnesium concentrations. Biochemistry *38*, 5572–5581.
63. Sondhi, D., and Cole, P.A. (1999). Domain interactions in protein tyrosine kinase Csk. Biochemistry *38*, 11147–11155.
64. Vang, T., Tasken, K., Skalhegg, B.S., Hansson, V., and Levy, F.O. (1998). Kinetic properties of the C-terminal Src kinase, p50csk. Biochim. Biophys. Acta *1384*, 285–293.
65. Ablooglu, A.J., and Kohanski, R.A. (2001). Activation of the insulin receptor's kinase domain changes the rate-determining step of substrate phosphorylation. Biochemistry *40*, 504–513.
66. Ablooglu, A.J., Frankel, M., Rusinova, E., Ross, J.B., and Kohanski, R.A. (2001). Multiple activation loop conformations and their regulatory properties in the insulin receptor's kinase domain. J. Biol. Chem. *276*, 46933–46940.
67. Barker, S.C., Kassel, D.B., Weigl, D., Huang, X., Luther, M.A., and Knight, W.B. (1995). Characterization of pp60c-src tyrosine kinase activities using a continuous assay: autoactivation of the enzyme is an intermolecular autophosphorylation process. Biochemistry *34*, 14843–14851.
68. Boerner, R.J., Kassel, D.B., Edison, A.M., and Knight, W.B. (1995). Examination of the dephosphorylation reactions catalyzed by pp60c-src tyrosine kinase explores the roles of autophosphorylation and SH2 ligand binding. Biochemistry *34*, 14852–14860.
69. Boerner, R.J., Consler, T.G., Gampe, R.T., Jr., Weigl, D., Willard, D.H., Davis, D.G., Edison, A.M., Loganzo, F., Jr., Kassel, D.B., Xu, R.X., et al. (1995). Catalytic activity of the SH2 domain of human pp60c-src; evidence from NMR, mass spectrometry, site-directed mutagenesis and kinetic studies for an inherent phosphatase activity. Biochemistry *34*, 15351–15358.
70. Boerner, R.J., Barker, S.C., and Knight, W.B. (1995). Kinetic mechanisms of the forward and reverse pp60c-src tyrosine kinase reactions. Biochemistry *34*, 16419–16423.
71. Edison, A.M., Barker, S.C., Kassel, D.B., Luther, M.A., and Knight, W.B. (1995). Exploration of the sequence specificity of pp60c-src tyrosine kinase. Minimal peptide sequence required for maximal activity. J. Biol. Chem. *270*, 27112–27115.
72. Wong, T.W., and Goldberg, A.R. (1984). Kinetics and mechanism of angiotensin phosphorylation by the transforming gene product of Rous sarcoma virus. J. Biol. Chem. *259*, 3127–3131.
73. Milligan, J.F., Groebe, D.R., Witherell, G.W., and Uhlenbeck, O.C. (1987). Oligoribonucleotide synthesis using T7 RNA polymerase and synthetic DNA templates. Nucleic Acids Res. *15*, 8783–8798.
74. Yan, M., and Templeton, D.J. (1994). Identification of 2 serine residues of MEK-1 that are differentially phosphorylated during activation by raf and MEK kinase. J. Biol. Chem. *269*, 19067–19073.
75. Zheng, C.F., and Guan, K.L. (1993). Properties of MEKs, the kinases that phosphorylate and activate the extracellular signal-regulated kinases. J. Biol. Chem. *268*, 23933–23939.
76. Breaker, R.R. (2002). Engineered allosteric ribozymes as biosensor components. Curr. Opin. Biotechnol. *13*, 31–39.
77. Huynh, Q.K., Kishore, N., Mathialagan, S., Donnelly, A.M., and Tripp, C.S. (2002). Kinetic mechanisms of IkappaB-related kinases (IKK) inducible IKK and TBK-1 differ from IKK-1/IKK-2 heterodimer. J. Biol. Chem. *277*, 12550–12558.